Hydrostatic Force Sensor for Robotic Applications

H. Kazerooni,[1] Mark S. Evans,[2] and J. Jones[1]

This article presents a theoretical and experimental investigation of a new kind of force sensor which detects forces by measuring an induced pressure change in a material of large Poisson's ratio. In this investigation, we develop mathematical expressions for the sensor's sensitivity and bandwidth, and show that its sensitivity can be much larger and its bandwidth is usually smaller than those of existing strain-gage-type sensors. This force sensor is well-suited for measuring large but slowly varying forces. It can be installed in a space smaller than that required for existing sensors. This paper also discusses the effects of various parameters on the sensor's performance and on failure modes. To verify the theoretical derivation, a prototype force sensor was designed and built. This prototype hydrostatic force sensor can measure the compressive forces up to 7200 lbf and tensile forces up to 3500 lbf.

Nomenclature

- A_f = area of the fluid
- A_s = effective cross-sectional area of the screw
- B = bulk modulus
- E_s = Young's modulus for screw
- f = force to be measured (it is a positive quantity for tensile forces and negative for compressive forces)
- f_i = pre-load force provided by n screws (always a positive quantity)
- f_{max} = maximum operating force: 3500 lbf (tensile force)
- f_{min} = minimum operating force: −7200 lbf (compression force)
- f_s = screw force (it is a positive quantity for tensile forces and negative for compressive forces)
- h = fluid height in the sensor
- K_f = fluid stiffness
- K_s = screw stiffness
- K_t = force sensor stiffness
- L_s = effective length of screw
- n = number of screws
- p = fluid pressure
- S = the force sensor sensitivity: volt/lbf
- S_p = the pressure sensor sensitivity: 1.34 mvolt/psi
- v = pressure transducer output voltage
- σ_s = screw stress: $\sigma_s = f_i/nA_s$
- σ_{all} = maximum allowable tensile stress in the screw: 135,000 psi
- σ_p = maximum allowable pressure for the force sensor: 5000 psi
- a, b, c, d, e, g, k = dimensions in Fig. 5 and Fig. 6

1 Introduction

Application of robotics to manufacturing tasks requires mechanical interaction with the environment or with the object being handled, in addition to high speed maneuvering in unconstrained space. For example, in a robotic assembly task whose objective is combining a number of individual parts into one completed device, the parts must be quickly assembled while avoiding damage to either the individual parts or the device. The very nature of the assembly process requires the robot (through the part) to contact the environment (the partially completed device). To successfully complete this constrained maneuver, the manipulator must develop compliant motion where the interaction force along the constrained direction is accommodated rather than resisted. Whitney [10] identifies six different approaches for robot force control. These six may be divided into two categories of compliant motion development: hybrid control and compliance control. The hybrid control method controls force and position in a nonconflicting way [6, 8] by commanding force along directions constrained by the environment and position along those directions in which the manipulator is unconstrained. The compliance control approach focuses on the relationship between the manipulator position, the commanded quantity, and the interaction force, a specified function of the command signal [3, 4, 5, 9]. With this approach, the designer can ensure that the manipulator will maneuver in a constrained space while maintaining an appropriate contact force. References [1] and [2] present valuable information on performance and application of various force and torque sensors for robotics applications.

The sensor proposed in this article detects a force by measuring an induced pressure change in a material of large Poisson's ratio [7] such as rubber. The method proposed for measuring applied forces is shown schematically in Fig. 1. In order to evaluate this sensor, we determine two of its properties: *sensitivity* and *bandwidth.* A sensor's "sensitivity" tells us the quality of the signal (i.e., its resolution; volt/lbf). A sensor's "bandwidth" tells us the range of force signal speeds that this force sensor can measure. Force sensors can record only the frequency components of the applied forces which fall within the sensors' bandwidth. If the bandwidth of the sensor is not wide in comparison with the bandwidth of the rest of the system (e.g., robot, actuation, etc.), either the force sensor dynamics must be mod-

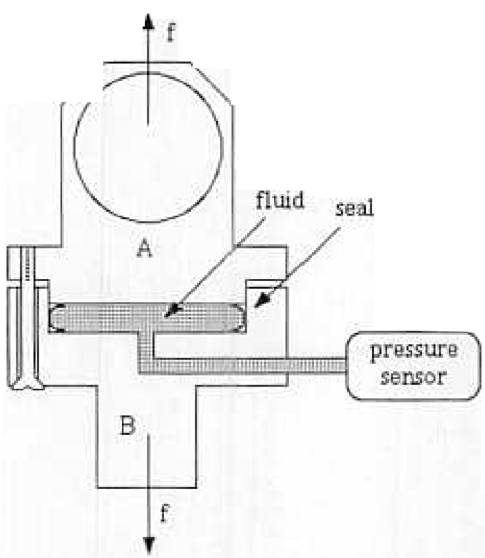

Fig. 1 Schematic of the hydrostatic sensor: the pressure increase in a high Poisson ratio material is a direct result of applied force. If load f is a tensile force, the fluid pressure decreases from the initial preload value. If load f is a compressive force, the fluid pressure increases.

[1] Mechanical Engineering Department, University of California at Berkeley, Berkeley, CA 94720.

[2] Mechanical Engineering Department, Brigham Young University, Provo, Utah 84602.

Contributed by the Dynamic Systems and Control Division of The American Society of Mechanical Engineers. Manuscript received by the DSCD July 13, 1994. Associate Technical Editor: C. W. de Silva.

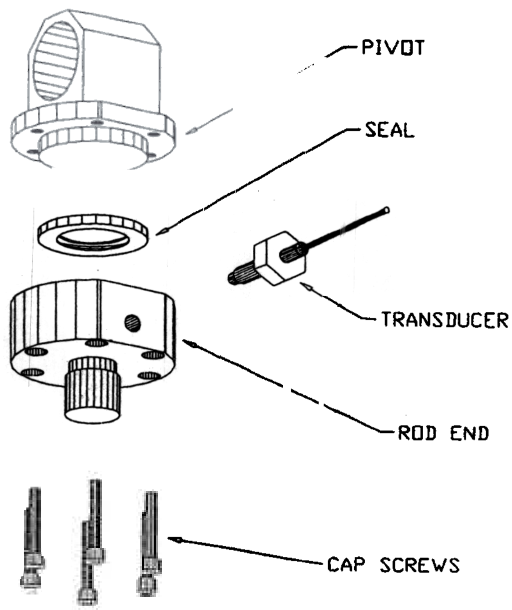

Fig. 2 An exploded view of the sensor

eled for controller design, or a lower bandwidth for overall control system should be considered.

2 Architecture

The objective is to design and construct a prototype hydrostatic force sensor to measure the compressive and tensile forces in one direction. Figure 1 shows a schematic of the sensor configuration. It consists of two components (part A and part B) that behave like a piston and a cylinder. The pressure in the fluid trapped between A and B is measured by a pressure transducer. A standard face seal prevents fluid leakage. Because this force sensor must measure both compression and tension, it is necessary to clamp part A and part B together with screws. The clamping force which we call preload, f_i, is applied by tightening the screws. The more the screws are tightened, the greater pre-load force that can be generated in the fluid. The force to be measured is f. If load f is a tensile force, the fluid pressure decreases from the initial pre-load value. If load f is a compressive force, the fluid pressure increases. Figure 2 shows an exploded view of this sensor. Figure 3 shows the sensor built at the University of California, Berkeley.

3 Design Procedure

The first step in the design procedure is to derive the constraints on the design parameters as inequalities. Then the performance specifications (i.e., sensitivity and bandwidth) are quantified as equalities. Designers can optimize the sensor design using the equalities while satisfying the constraint inequalities.

3.1 Design Constraints. The clamping force (preload f_i) is applied by tightening the screws. If a tensile force, f, is applied on the system, the screw force increases where as the fluid force (or the fluid pressure) decreases. Conversely, if a compressive force, f, is applied on the system, the screw force decreases and the fluid pressure increases. The screws and the fluid chamber act like two springs in parallel. The resulting screw force, f_s, and the fluid force, f_f, can be calculated from Eqs. (1) and (2).

$$f_s = f_i + \left(\frac{K_s}{K_s + K_f}\right) f \tag{1}$$

$$f_f = -f_i + \left(\frac{K_f}{K_s + K_f}\right) f \tag{2}$$

K_f and K_s are effective stiffness of the fluid and the screws and can be calculated from Eqs. (3) and (4).

$$K_f = \frac{BA_f}{h} \tag{3}$$

$$K_s = \frac{nA_sE_s}{L_s} \tag{4}$$

A_s, E_s, L_s, and n are the area, Young modulus, effective length, and quantity of the screws, respectively. B, A_f, and h are the bulk modulus, fluid surface area, and fluid height, respectively. The stress in the screws and the pressure in the fluid can be calculated from Eqs. (5) and (6).

$$\sigma_s = \frac{f_i}{nA_s} + \left(\frac{K_s}{K_s + K_f}\right) \frac{f}{nA_s} \tag{5}$$

$$p = -\frac{f_i}{A_f} + \left(\frac{K_f}{K_s + K_f}\right) \frac{f}{A_f} \tag{6}$$

It can be observed from Eqs. (5) and (6) that when $f = 0$ (i.e., there is no force on the force sensor), the forces in the fluid and the screws are both equal to f_i. When force f is applied as a tensile force (as shown in Fig. 1), the stress in the screw, σ_s, increases while the pressure in the fluid decreases. If f is a tensile force, there are two limiting situations that cause failure in the system:

Case 1: The stress in the screw, σ_s, reaches the material yield stress.
Case 2: The pressure in the fluid, p, decreases to zero.

If f is a compressive force, one other limiting situations can cause failure in the system:

Case 3: The pressure in the fluid, p, reaches the maximum measurable pressure of the pressure transducer or the maximum allowable pressure of the seal.

The designers must assure that the three limiting situations above never occur during normal system operation. Next we explain how to guarantee that these four cases do not occur.

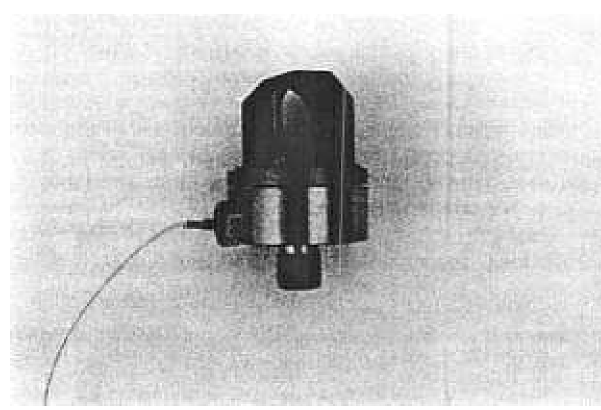

Fig. 3 A prototype force sensor is custom designed to fit a linear actuator.

Cases 1 and 2:

To guarantee that case 1 for a tensile force (i.e., failure of the screw material) does not occur, the designer must ensure that the screw stress, σ_s, remains below the maximum allowable screw stress, σ_{all}, when f_{max} is imposed on the system. This is shown in inequality 7, where it can be observed that choosing a small preload, f_i, helps the designers keep σ_s smaller than σ_{all}. On the other hand, to guarantee that case 2 (i.e., the fluid pressure becomes zero) does not occur, f_i should be chosen to be large enough to satisfy inequality 8.

$$\sigma_s = \frac{f_i}{nA_s} + \left(\frac{K_s}{K_s + K_f}\right)\frac{f_{max}}{nA_s} < \sigma_{all} \tag{7}$$

$$\frac{f_i}{A_f} + \left(\frac{K_f}{K_s + K_f}\right)\frac{f_{max}}{A_f} \quad 0 \tag{8}$$

$$\left(\frac{K_f}{K_s + K_f}\right) f_{max} \qquad \left(\frac{K_s}{K_s + K_f}\right) f_{max}$$

Inequality 9 is a design constraint which is necessary to prevent force sensor failure in the presence of the maximum tensile force, f_{max}.

Cases 3:

To guarantee that case 3 for a compressive force (i.e., excessive fluid pressure) does not occur, the designer must ensure that the fluid pressure, p, does not reach the maximum allowable pressure of the pressure transducer, σ_p, when f_{min} is imposed on the system. Note that f_{min} is a negative quantity; for the prototype force sensor $f_{min} = -7200$ lb.) As seen in inequality 10, this can be ensured by choosing a small preload, f_i.

$$-\frac{f_i}{A_f} + \left(\frac{K_f}{K_s + K_f}\right)\frac{f_{min}}{A_f} \tag{10}$$

Solving for f_i from inequality 10 results in an upper bound for the preload, f_i during compression.

$$f_i < \sigma_p A_f + \left(\frac{K_f}{K_s + K_f}\right. \tag{11}$$

Inequalities 9 and 11 must be satisfied to prevent sensor failure.

3.2 Design Parameters. *Sensitivity* and *bandwidth*, are two major parameters of this sensor. The sensitivity of a sensor represents the quality of the signal (i.e., its resolution in volt/lbf) wherein the bandwidth represents the range of force signal speeds that this force sensor can measure. One always requires a sensor that can respond to high frequency signals with high resolution. Force sensors can record only the frequency components of the applied forces which fall within the sensors' bandwidth. If the bandwidth of the sensor is not wide in comparison with the bandwidth of the rest of the system (e.g., robot, actuation, etc.), either the force sensor dynamics must be modeled for controller design, or a lower bandwidth for overall control system should be considered.

The pressure in the fluid can be calculated via Eq. (6) and it is rewritten here in a more appropriate form.

$$p = \frac{K_f}{K_s + K_f}\frac{1}{A_f}\left(f - \frac{K_s + K_f}{K_f} f_i\right) \tag{12}$$

[3] Note that σ_p must be chosen to be the smallest of the maximum measurable pressure of the pressure transducer or the maximum allowable pressure of the seal.

Since the voltage of the pressure transducer, v, is proportional to the pressure increase, Eq. (13) applies.

$$v = S_p p \tag{13}$$

S_p is the pressure transducer sensitivity. Substituting Eq. (12) into (13) results in the output voltage as a function of the applied force.

$$\frac{K_f}{K_s + K_f}\frac{S_p}{A_f}$$

The force sensor sensitivity therefore equals

$$S = \tag{15}$$

Designers always wish to have a large sensitivity in the sensor: a large sensitivity in the force sensor results in a large voltage for a given applied force. The parameters of Eq. (15) can be chosen to yield a particular sensitivity. On the other hand, the designer should be aware of the role of the design parameters on another important sensor property: bandwidth. The overall bandwidth of a robotic system is limited by high-frequency unmodeled dynamics (e.g., structural resonances for bending and torsion, sensor dynamics, actuator dynamics). To achieve a wide bandwidth for the closed-loop system, it is necessary to consider high order dynamics in modeling the system. Adding high order dynamics to the system results in a wider bandwidth for the system at the expense of a high order compensator. If higher order dynamics cannot be determined, it is necessary to compromise on the overall system bandwidth. It is usually recommended to "push" the high frequency unmodeled dynamics by designing "stiff" components. In other words, a robot's components must be designed to have large natural frequencies. The natural frequency or bandwidth of a sensor can be calculated from Eq. (16).

$$\omega \cong \left[\frac{K_t}{m}\right]^{1/2}$$

K_t is the stiffness of the sensor and m is some effective mass which depends on the rest of the robot inertia. It is rather impractical to arrive at the natural frequency of the force sensor without any regard for the inertia of the other components. We leave Eq. (16) without further development, since m is a function of robot inertia. However, we must consider that the larger the stiffness of the sensor, the larger the natural frequency is. The total stiffness of the pressure transducer can be derived from Eq. (17).

$$Kt = K_s + K_f \tag{17}$$

To achieve a large stiffness, both K_s and K_f must be large. From Eq. (15) it can be observed that a large sensitivity requires a small A_f, but Eq. (3) shows that a small A_f results in a low fluid stiffness. One method of dealing with this tradeoff is to decrease h, so K_f does not get too small. Another tradeoff is the screw stiffness: a large screw stiffness results in a large total stiffness of the system, but this decreases the system sensitivity. Equation (15) shows that stiff screws decrease the system sensitivity. We recommend that, for low bandwidth yet still precise operation, the designer choose a set of screws with small stiffness. On the other hand, in wide bandwidth operations, we recommend a large stiffness for the screws.

Example:

$B = 7.19 \times 10^5$ psi for glycerin
$A_f = 1.767$ in.^{2} (diameter: 1.5 in.)
$h = 0.123$ in.
$n = 6$

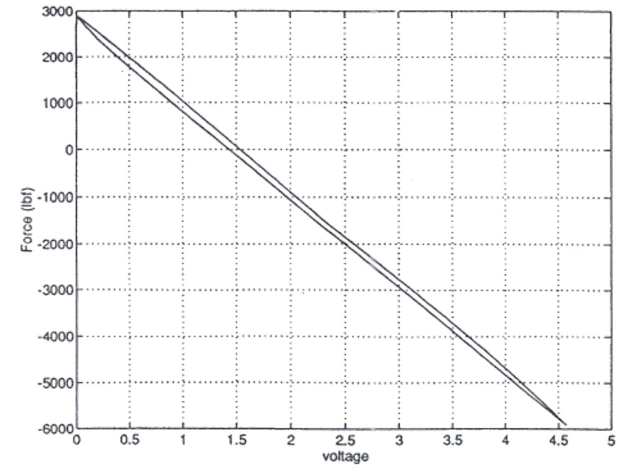

Fig. 4 Experimental plot of the sensor performance; the slope of the curve depicts the experimental value for the sensor sensitivity

$$
\begin{aligned}
A_s &= 0.014 \text{ in.}^2 \text{ (\#8-32 UNC)} \\
E_s &= 1.9 \times 10^7 \text{ psi (Titanium, Grade 5)} \\
L_s &= 0.725 \text{ in.} \\
\sigma_{all} &= 135 \text{ ksi (Titanium, Grade 5)} \\
f_{max} &= 3{,}500 \text{ lbf} \\
f_{min} &= -7{,}200 \text{ lbf} \\
S_p &= 1.34 \times 10^{-3} \text{ volts/psi}^4 \\
K_f &= 1.01 \times 10^7 \text{ psi (from Eq. (3))} \\
K_s &= 2.2 \times 10^6 \text{ psi (from Eq. (4))}
\end{aligned}
$$

Substituting the above values into inequalities 9 and 11 results in the following two inequalities.

$$2{,}874 \text{ lbf} < f_i < 10{,}073 \text{ lbf}$$

$$f_i < 2923 \text{ lbf}$$

We choose f_i to be 2900 lbf. Substituting the above data, the sensor sensitivity and stiffness are:

$$S = 6.22708 \times 10^{-4} \text{ volts/lbf} \quad \text{(from Eq.(15))}$$

$$K_t = .8128 \times 10^6 \text{ lbf/in.} \quad \text{(from eq. (17))}$$

Figure 4 shows the experimental plot of the system performance where the slope of the curve depicts the experimental value for the sensor sensitivity. The hysteresis comes from the seal in the force sensor.

$$S_{experimental} = 5.260 \times 10^{-4} \text{ volts/lbf}$$

4 Design Concerns

4.1 Sealing. A major design problem involves the sealing of the fluid within the chamber while allowing for some small but necessary motion in the axial direction. This is achieved by using a standard face seal. The seal, which is spring-energized Teflon, is rated to over 10,000 psi with the proper surface finish on the mating parts. The spring stiffness in this seal is small in comparison with the fluid stiffness.

The concern is that the seal should not be compressed to be shorter than its minimum recommended value. To guarantee that the seal never reaches its minimum value, the following inequality must be guaranteed in regrad to Figure 5:

$$b_{min} = d_{max} - a_{min} \tag{18}$$

We choose the tolerances on a and d such that b_{min} always remains larger than the minimum recommended height of the seal.

$$b_{min} = 0.3250'' - 0.2030'' = 0.12200'' \tag{19}$$

The minimum seal height is 0.121″, so the seal is safe.

When compressive forces are imposed on the force sensor, the seal extrudes into the gap (g in Fig. 6). Release of force traps and crushes the extruded portion of the seal between the hardware surfaces. If the gap, g, is too large, repeated pressure cycles will "nibble" away at the seal resulting in early failure.

The finish of the surfaces over which the seal must slide, greatly influences the performance of the seal. A rough surface finish wears the seal cover material too rapidly. Extremely smooth surfaces result in insufficient material transfer to form a thin film. The seal manufacturer commends a surface finish of 8 microin.

4.2 Lateral Stability of the Sensor. An eccentric load could cause the sensor to buckle or possibly bind. To prevent this, the tolerances on the clearance of the cylinder and piston, as well as the position of the pivot and the mating threads have been tightly toleranced. The tight tolerance on the clearance of the bore of the cylinder also prevents the extrusion of the Teflon seal material into the gap under the high pressure. The maximum and minimum gap between the piston and cylinder (shown by g_{max} and g_{min} in Fig. 6) in the presence of manufacturing uncertainties can be calculated by:

$$g_{max} = k_{max} - e_{min} \tag{21}$$

$$g_{min} = k_{min} - e_{max} \tag{22}$$

We choose the tolerances on e and k such that the clearance between the cylinder and piston will be an ANSI Locational Fit, LC3.

$$g_{max} = 1.5010'' - 1.4990'' = 0.0020'' \tag{23}$$

$$g_{min} = 1.5005'' - 1.4995'' = 0.0010'' \tag{24}$$

4.3 Assembly Procedure. The assembly begins by covering the seal and threaded end of the transducer with fluid. It is very important that there are no air bubbles in the fluid when the chamber is sealed, so a syringe is used to inject fluid into the tight areas of the seal. The entire surface of the chamber on the rod end part is then coated with glycerin, and the seal is installed. The transducer is screwed in to be finger-tight. Then an excessive amount of fluid is added to the chamber. At this point any visible air bubbles are removed from the fluid in the chamber with the syringe. The pivot is then slowly inserted into

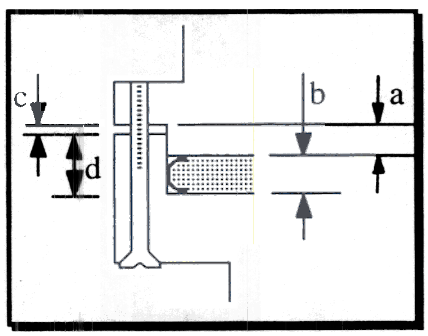

Fig. 5 The sensor must be designed such that c becomes zero before the seal reaches its recommended minimum height

[4] This number is calculated based on the data sheets from the pressure sensor: Sp = (pressure sensor gain) × (amplifier gain: 50) = 1.34 mv/psi.

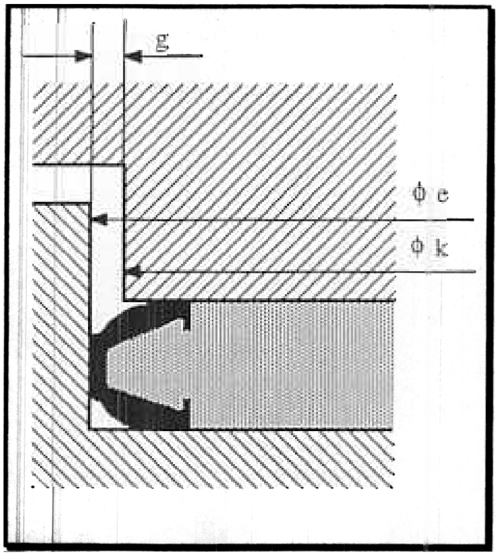

Fig. 6 The diameters e and k should be designed to give the ANC? Locational fit, LC3

the rod end part by hand. Fluid should slowly bleed up between the two parts until it is difficult to insert the pivot end any further. The six screws are then inserted and tightened in a cross pattern while watching the pressure output of the transducer. At several points while tightening the screws to the proper preload, it is necessary to tighten the transducer body to ensure a good seal at its base. Also, while tightening the preload screws, the width of the gap between the flanges of the rod end and pivot parts is measured to ensure that an even tightening procedure is taking place. This procedure is continued until the output of the transducer shows that the proper preload has been applied.

5 Conclusion

This article presents a theoretical and experimental investigation of a new kind of force sensor which detects forces by measuring an induced pressure change in a material of large Poisson's ratio. This force sensor is well-suited for measuring large but slowly varying forces. It can be installed in a space smaller than that required by existing sensors. Based on our theoretical and experimental investigations, we have shown that the sensor sensitivity can be much larger and its bandwidth is usually smaller than those of existing strain-gage-type sensors. To verify the theoretical derivation, a prototype force sensor was designed and built. This prototype hydrostatic force sensor can measure the compressive forces up to 7200 lbf and tensile forces up to 3500 lbf.

References

1 de Silva, C. C., *Control Sensors and Actuator*, Printice Hall, 1989.

2 Dally, J. W., Riley, W. F., and McConnell, K. G., *Instrumentation for Engineering Measurements*, Wiley, New York, 1984.

3 Hogan, N. "Impedance Control: An Approach to Manipulation, Part I—Theory, Part II—Implementation, Part III, Applications," ASME Journal of Dynamic Systems, Measurement, and Control, pp. 1–24, June 1985.

4 Kazerooni, H., Waibel, B., "On the Stability of the Constrained Robotic Maneuvers in the Presence of Modeling Uncertainties," *IEEE Transaction on Robotics and Automation*, Vol. 7, No. 1, Feb. 1991.

5 Kazerooni, H., Tsay, T. I., and Hollerbach, K., "A Controller Design Framework for Telerobotic Systems," *IEEE Transaction on Control Systems Technology*, Vol. 1, No. 1, Mar. 1993.

6 Mason, M. T., "Compliance and Force Control for Computer Controlled Manipulators," *IEEE Trans. on Systems, Man, and Cybernetics*, SMC-11(6) pp. 418–432, 1981.

7 McClintock, F., and Argon, A., *Mechanical Behavior of Materials*, Addison-Wesley Publishing Company, 1966.

8 Raibert, M. H., and Craig, J. J., "Hybrid Position/Force Control of Manip." ASME Journal of Dynamics Systems Measurement, and Control, Vol. 102, pp. 126–133, 1981.

9 Salisbury, K. J., "Active Stiffness Control of a Manipulator in Cartesian Coordinates," *Proc. 19th IEEE Conference on Decision and Control*, Albuguerque, 95–100, Dec. 1980.

10 Whitney, D. E., "Historical Perspective and State of the Art in Robot Force Control," The *International Journal of Robotics Research*, Vol. 6(1), pp. 3–14, 1987.

Kalman Filtering Error Due to Inaccuracy in Filter's Initial Condition

Z. Gajic[1] and J. Boka[2,3]

It is a very well known fact that the initial condition of the optimal linear Kalman filter has to be set at the mean value of the system initial state. In this paper, we have derived an expression for the filtering error in the case when this condition is not satisfied. Both continuous- and discrete-time domain filters are considered. The obtained results are simple and elegant and clearly indicate the effect of the erroneous filter's initial condition. An example is included in order to demonstrate the results obtained.

1 Introduction

In this paper we study the problem of the Kalman filter (Kalman, 1960) error due to inaccuracy in the filter's initial condition. Both the continuous- and discrete-time problems are considered. It has been shown in both cases that the corresponding error effects only the optimal Kalman filter transient response. This error can be obtained from the Lyapunov differential (difference) equation, whose solution under the standard stabilizability-detectability conditions tends to zero at steady state (asymptotic stability). Hence, the optimal Kalman filter performance at steady state is unchanged due to its initial condition inaccuracy.

Several authors studied similar problems in the past. The effect of errors in the covariance matrix of the Kalman filter's initial state was studied by Nishimura (1966) and Heffes (1966) in the discrete-time domain. In Nishimura (1966) no measurement noise problem had been considered; even more, no initial conditions were imposed neither on the system nor the filter. Heffes (1966) had included the measurement noise, and studied the effect of the optimal filter gain perturbation due to inaccuracies in the initial covariance matrix and incorrect noise models without imposing any value on the filter's initial condition so that his problem formulation and obtained results are different from what is presented in this paper. Namely, we study the problem when the initial condition of the Kalman filter is not set at the mean value of the system initial state (Kalman, 1960), so that the optimization has to be performed with respect to both the variance of the estimation error and the mean value of

[1] Rutgers University, Department of Electrical and Computer Engineering, Piscataway, NJ 08855-0909.

[2] Martin Marietta Astro Space, Princeton, NJ 08540.

[3] The work of the second author was performed while he was a graduate student at Rutgers University, Department of Mechanical and Aerospace Engineering.

Contributed by the Dynamic Systems and Control Division of The American Society of Mechanical Engineers. Manuscript received by the DSCD March 28, 1995. Associate Technical Editor: O. Nwokah.